Journal of Plastic, Reconstructive & Aesthetic Surgery (2019) 72, 831–841

JPRAS
An International Journal of Surgical Reconstruction
www.JPRASurg.com

"Radiological morphometric analysis of the zygomatic arch: Application of osteosynthesis on the upper arch border for rigid fixation"

Hyonsurk Kim[a], **Jeongmin Yoon**[b], **Byung-il Lee**[b,*]

[a] *Department of Plastic and Reconstructive Surgery, Dankook University Hospital, Dankook University College of Medicine, 201 Manghyang-ro, Dongnam-gu, Cheonan-si, Chungcheongnam-do 31116, Republic of Korea*
[b] *Department of Plastic and Reconstructive Surgery, Korea University Anam Hospital, Korea University College of Medicine 73, Inchon-ro, Seongbuk-gu, Seoul 02841, Republic of Korea*

Received 7 September 2018; accepted 18 November 2018

KEYWORDS
Zygomatic arch fracture;
Zygomatic arch morphometry;
Zygomatic arch fracture open reduction and internal fixation;
Zygomatic arch tangential fixation

Abstract *Background:* This study was designed to introduce a novel method of applying osteosynthetic materials to the upper zygomatic arch border for fracture fixation through a temporal incision, and analyze the radiologic morphometric dimensions of the arch to verify its validity.
Methods: Radiological morphometry was analyzed in 51 adult patients with unilateral isolated zygomatic arch fractures. Frequent fracture sites, sites of minimal thickness and height, and their correlation were evaluated, as were the locations and dimensions of fixation vantage points. The novel surgical method based on the results was implemented in 17 clinical cases.
Results: Frequent fracture sites, occurring 4.40, 16.47 and 30.48 mm posterior to the arch origin, did not correlate to sites of minimal height and thickness. Arch minimal thickness and height locations were 12.23 and 27.09 mm behind its origin, respectively. Fixation vantage point dimensions varied from point to point, with upper thickness ranging from 1.67 to 4.86 mm and mid-portion thickness ranging from 2.06 to 7.36 mm, and height ranging from 8.99 to 22.53 mm. Arch vertical axis inclination ranged from 6.51° to 16.47°, which increased as the arch stretches posteriorly. These results suggested the use of 1.5 mm-wide plates and 1 mm-diameter screws with 6–8 mm length. Patients received surgery based on these morphometry results for satisfactory stabilization.

* Corresponding author.
E-mail address: guro@korea.ac.kr (B.-i. Lee).

https://doi.org/10.1016/j.bjps.2018.11.014

Conclusions: This study introduces a new method for open reduction and internal fixation of arch fractures, with morphometric analysis of the arch verifying the validity of tangential plate application to the upper border.

Introduction

In most zygomatic arch fractures, including zygomaticomaxillary complex fractures involving the arch, the well-known Gillies or Keen (intraoral) methods are sufficient for stable reduction.[1] However, open reduction is generally considered for unstable or laterally displaced fractures.[2]

Previous open reduction methods generally used a coronal or endoscopic approach to apply hardware to the outer cortex of the arch, which could be palpated through the skin and also increase facial width. Other drawbacks of these methods included prolonged operative times, lengthy scalp scars, and the need for technical proficiency in using additional equipment.

The authors have devised and implemented a new method for the management of arch fractures that can overcome these drawbacks. Under direct vision through a temporal hairline incision, the authors tangentially applied osteosynthetic material to the upper border. As a prerequisite for clinically applying this method, the authors also performed an analysis of arch radiological morphometry. This study hereby provides reference data for surgical management of acute arch fractures, secondary correction of old arch fractures with malunion, and aesthetic arch procedures that aim to improve facial contour.

Methods & materials

Materials

The radiologic morphometry study included 51 adult patients admitted to Korea University Anam Hospital for zygomatic arch fractures between January 2008 and August 2014. All patients had 2 mm-thick axial and coronal slice CT scans with 3D reconstruction, and three distinctly visible fracture lines and two fractured bone segments on the CT images. Patients with zygomaticomaxillary complex fractures were excluded except for partial zygoma body fractures in which the anteriormost fracture line upper end was located within the boundaries of the arch and not on the zygoma body. The novel surgical method was implemented in 17 cases. Ethics approval was obtained at the Korea University institutional review board (K2017-3229).

Methods

Morphometry study included evaluation of frequent fracture sites, sites of minimal arch thickness and height, and their correlation. The location and dimensions of vantage points for fixation were also included. Each assessment was performed, repeated thrice at different times, and averaged by the senior author to ensure reliability.

Frequent fracture sites

A reference guideline was established on lateral view 3D CT scans for measuring the position of fracture sites in anterior-posterior dimensions. This guideline ('G-line') was set perpendicular to the Frankfort horizontal line, passing through the point where the upper border of the zygomatic arch shifts from a horizontal to vertical slope. Points corresponding to this G-line on 2D axial slices were used as a reference for fracture position measurement. Since arch fractures frequently present as oblique lines on lateral views, the distance from the reference point to the vertical mid-point of each fracture line was measured. This was done by choosing a 2D axial slice corresponding to this mid-point, then measuring the anterior-posterior distance between the G-line reference point and the midpoint of the fracture site outer and inner cortices on this axial slice using PiVIEWSTAR®(version 5.0.9.58, Infinitt, Seoul, Korea) software. The anteriormost fracture line was designated as Fa, the middle line as Fm, and the posterior fracture line Fp; the horizontal distance from the G-line to these sites was measured to verify frequently fractured locations (Figure 1).

Correlation of arch minimal height, thickness and fracture sites

Points of minimal vertical height and horizontal thickness, expected to be prone to fracture, were verified on 2D coronal slices and the distance to the G-line measured on corresponding axial slices. The correlation between these sites and Fa, Fm and Fp were analyzed.

Vantage points for screw insertion

Vantage points for screw insertion were selected in reference to fracture sites, and arch thickness and height were measured at these points to ensure secure tangential screw insertion. Fracture management principles generally require at least one screw inserted on both sides of a fracture line for secure fixation, and since in most segments the middle portion is a physically balanced location for screw insertion, these midpoints were designated as vantage points; axial slices corresponding to 3D images were used to measure the distance from the G-line to the midpoint of the anterior segment (between Fa and Fm), designated as P2, and the midpoint of the posterior segment (between Fm and Fp) designated as P3. P1 was set anterior to Fa at a distance equivalent to that between Fa and P2, and P4 was set posterior to Fp at a distance equivalent to the distance between Fp and P3. In cases where P1 was located on the body, it was designated as P1B; arch-located P1 points were designated P1A. The distance between the G-line and these points was measured. These points being the minimal screw insertion points for fixation, the thickness (width) of the upper, middle and lower portion at each point (designated on axial slices) and height were measured on 2D coronal slices

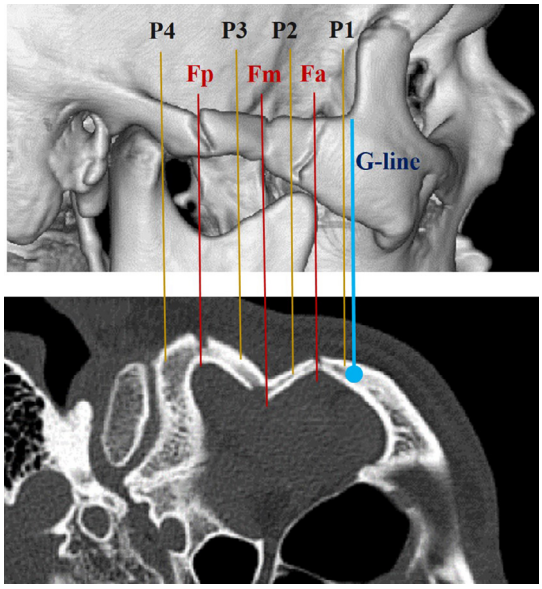

Figure 1 Landmarks used for Morphometry evaluation. G-line, virtual origin of the arch; Fa, anterior fracture line; Fm, middle fracture line; Fp, posterior fracture line; P2, midpoint between Fa and Fm; P3, midpoint between Fm and Fp; P1, anterior to Fa at a distance equivalent to that from Fa and P2; P4, posterior to Fp at a distance equivalent to that from Fp and P3.

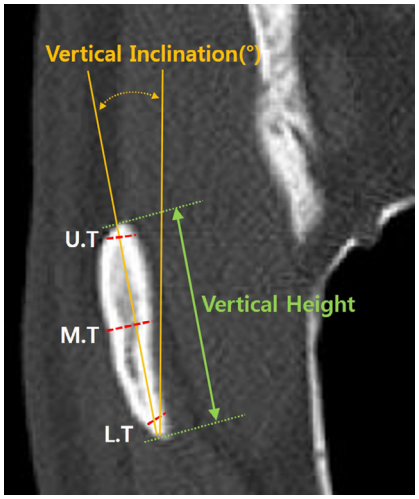

Figure 2 Thickness, vertical height, and vertical inclination of Zygomatic Arch. The upper, mid-, and lower thickness of the arch were measured at 1 mm below the upper border, the mid-portion of vertical height, and 1 mm above the lower border, respectively. Vertical inclination was measured as the angle between the arch vertical axis and facial CT vertical line. U.T, upper thickness; M.T, mid-thickness; L.T, lower thickness. (For interpretation of the references to colour in this figure legend, the reader is referred to the web version of this article.)

as reference values for screw and plate dimensions. Arch height was measured along the axis connecting the upper and lower arch border. Upper thickness was measured 1 mm below the upper arch border to anticipate cortical burring, middle portion thickness was measured at the vertical midpoint, and lower portion thickness 1 mm above the lower border.

Arch cross-sectional vertical axis inclination at each P point was also evaluated on coronal slices as a reference for directing screw insertion to avoid protrusion. Since fracture displacement distorts axis inclination, the corresponding points for P1A, P2 and P3 on the contralateral uninjured arch were used for analysis.

Height, lower thickness and axis inclination were not measured at P1B, along with P4 lower thickness and inclination, since these sites were regarded to have more than sufficient dimensions (Figure 2).

Statistical analysis

All statistics were determined using SPSS version 20.0 (SPSS Inc., Chicago, IL, USA). A series of one-way ANOVA test with Welch analysis for variance were run to compare means. This was followed by post hoc Dunnett T3 analyses to determine statistically significant differences ($p < 0.05$).

Patients and surgical procedure

Under general anesthesia, a 4.0 cm zigzag incision was made parallel and 1.5 cm superior to the temporal hairline. Subsequent dissection followed conventional coronal approach methods, under direct vision aided by a light source attached-retractor. Arriving 1.0 cm cephalad to the arch upper border, a horizontal incision was made in the deep temporal fascia superficial layer and the arch upper border exposed. The periosteum was incised with minimal fracture site subperiosteal dissection. After anatomical reduction, the upper border was lightly burred (approximately 1 mm) to a flat surface before tangentially applying plate and screws. 1.5 mm-width plates were used, narrower than or similar to the arch width. 1 mm-diameter screws with a length sufficient to span at least half of the vertical height of each fixation point were selected. Plates were molded to match the curvature of the contralateral uninjured arch on 2D axial slices. Screw fixation began with both anterior and posterior non-fractured portions and proceeded centrally towards each reduced segment held with a bone hook against the pull of the masseter. The insertion direction for each screw was matched to arch vertical axis inclination. At least one screw was inserted on either side of each fracture line, with additional screws inserted when more stability was required against anticipated masseter pull. After confirming stable fixation, the superficial layer of the deep temporal fascia was sutured to ensure periosteal continuity, and the superficial temporal fascia and scalp subsequently repaired (see Video 1). Post-operative radiologic imagery was regularly repeated every 2 weeks up to 6 weeks.

Results

The demographics of case patients are summarized in Table 1.

Frequent fracture sites

The mid-portion of Fa impinged obliquely onto the lateral zygoma body in almost half of the cases, and in extreme

Table 1 Demographic characteristics of patients.

Variables	Radiological study($n=51$)	Operative study($n=17$)
Age		
Mean ± SD, yr	46.8 ± 14.3	42.9 ± 13.0
Sex		
Male (%)	38 (74.5)	12 (70.6)
Female (%)	13 (25.5)	5 (29.4)
Side		
Right (%)	16 (31.4)	8 (47.1)
Left (%)	35 (68.6)	9 (52.9)
Type of fracture		
Arch only (%)	51 (100)	10 (58.8)
Complex (%)		7 (41.2)

Table 2 Distances between G-line and the sites of fractures, minimal vertical height, and minimal thickness.

Variables	Fa	Fm	Fp	VH	HT
Mean (mm)	4.40	16.47	30.48	27.09	12.23
Standard deviation (mm)	3.399	4.008	2.570	4.411	3.134
Standard error (mm)	0.476	0.561	0.360	0.618	0.439
95% CI for the mean (mm)	3.44-5.35	15.34-17.60	29.75-31.20	25.85-28.33	11.35-13.11
Minimal value (mm)	−4.23	9.86	23.03	21.05	8.01
Maximal value (mm)	10.88	30.27	36.61	43.10	26.88
P value	0.000 (in comparison between any sites)				

CI, Confidence intervals; Fa, Anterior fracture site; Fm, Middle fracture site; Fp, Posterior fracture site; VH, Site of minimal vertical height; HT, Site of minimal horizontal thickness.

cases Fa occurred 5 mm anterior to the G-line. In average, Fa was 4.40 mm posterior to the G-line. Fm and Fp were at an average 16.47 and 30.48 mm posterior to the G-line, respectively, with significant difference between each fracture location. Based on these findings, anterior fracture segments were a mean 12.07 mm long, while posterior segments were rather longer at 14.01 mm (Table 2, Figure 3).

Correlation of arch minimal height, thickness and fracture sites

Arch minimal vertical height and horizontal thickness (width) were 27.09 and 12.23 mm posterior to the G-line, respectively. However, both of these locations presented significant difference from frequently fractured sites, indicating that minimal height or thickness did not have a direct correlation to fracture occurrence sites (Table 2, Figure 3).

Vantage points for screw insertion

Table 3 summarizes the data concerning screw insertion vantage points for rigid fixation.

(1) Distance between G-line and P-points

The mean distance from P1B to the G-line was −4.73 mm, placing P1B on the lateral portion of the orbital rim. P1A was an average 1.67 mm posterior to the G-line, P2 10.43 mm, and P3 and P4 an average 23.49 and 37.31 mm posterior to the G-line, respectively (Table 4, Figure 4).

(2) Vertical height of P-points

The average vertical height of the arch at P1A was 22.53 mm, P2 16.56 mm, P3 9.18 mm, and P4 8.99 mm, displaying a gradual decrease in height as the arch stretches back. However, there was no significant difference between arch height at P3 and P4 (Figure 5).

(3) Horizontal thickness of P-points

The thickness of the arch at each point varied according to vertical location (Figure 6). Upper portion thickness ranged from 1.67 to 4.86 mm, with P1A having the greatest average thickness at 4.11 mm, and P2 being the least thick at 1.94 mm. Significant difference existed between the average thickness of each point, however the upper thicknesses of P3 and P4 displayed no significant difference, being 2.40 and 2.49 mm, respectively (Table 5).

Mid-portion thickness ranged from 2.06 to 7.36 mm. The average thickness was greatest at P4, being 5.60 mm, followed by P1B at 5.50 mm. P2 displayed the least mean thickness at 3.38 mm, and P3 also was relatively thin at 3.96 mm. Although the thickness of P1B and P1A were not significantly different, the thickness of the other points all displayed significant difference from each other (Table 6).

Lower portion thickness ranged from 1.93 mm to 4.95 mm. Mean thickness was greatest at P1A (4.51 mm), compared to the thinnest P3 (2.47 mm). Heights of all

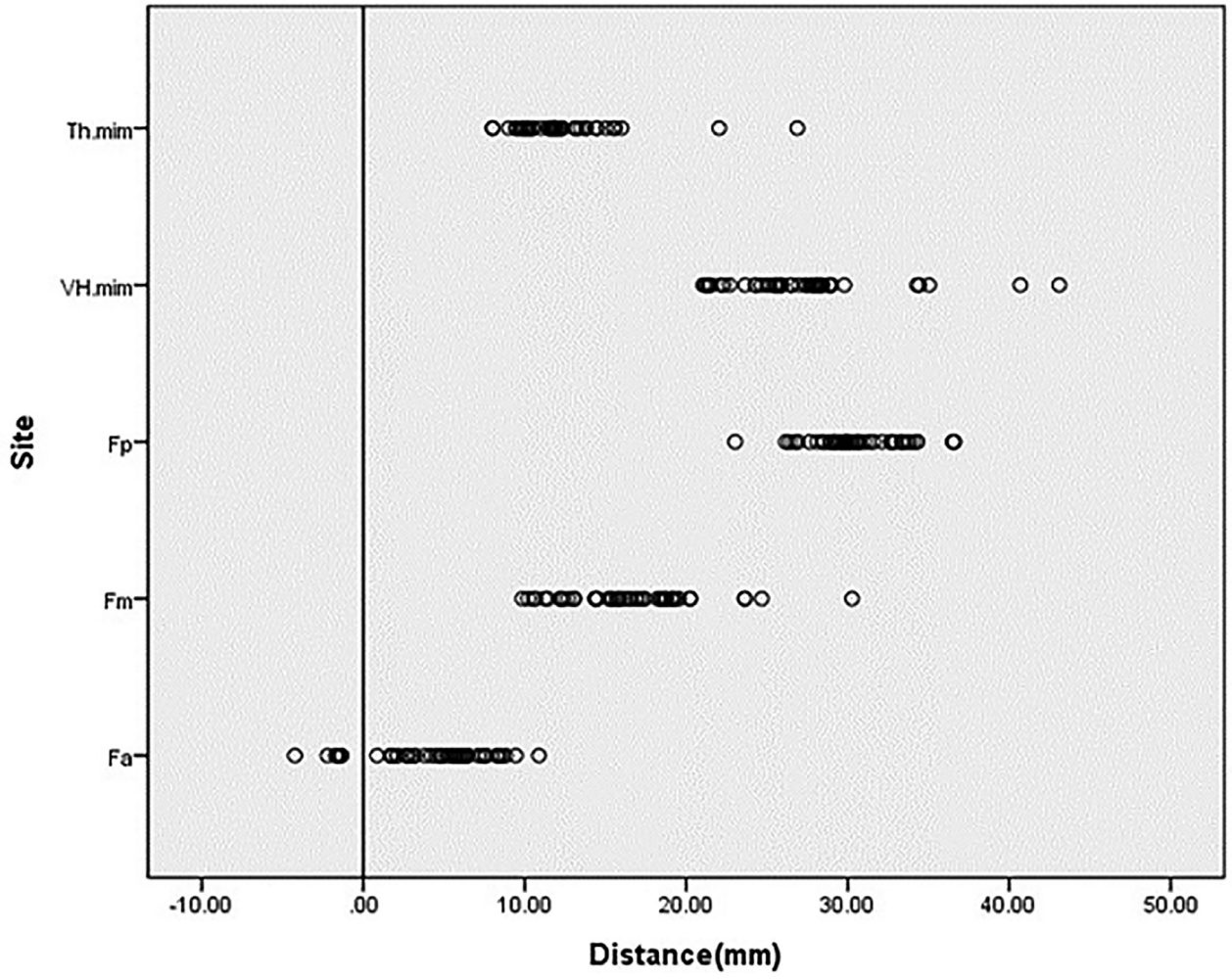

Figure 3 Distances between G-line and frequent fracture sites and sites of minimal height and thickness. Fa, anterior fracture site; Fm, middle fracture site; Fp, posterior fracture site; VH, site of minimal vertical height; HT, site of minimal horizontal thickness. The vertical line at 0.0 point represents the G-line. The distance to Fm was significantly longer than that to HT.

Table 3 Summary of the vantage points for rigid fixation with screw insertion.

Variables	P1B($n=25$)	P1A($n=26$)	P2($n=51$)	P3($n=51$)	P4($n=51$)
Distance from the G-line (mm)	−4.55	1.73	10.43	23.49	37.31
Vertical height (mm)		22.53	16.56	9.18	8.99
Thickness					
Upper border (mm)	3.04	4.11	1.94	2.40	2.50
Mid-level (mm)	5.50	4.83	3.38	3.96	6.00
Lower border (mm)		4.50	2.65	2.47	
Vertical inclination (°)		6.51	6.61	16.47	

P1B, Point 1 on zygomatic body; P1A, Point 1 on zygomatic arch.

three measured points were significantly different from each other (Table 7).

(4) Arch cross-section inclination

The arch vertical axis was inclined 6.51° and 6.61° medially at P1A and P2, respectively, with no significant difference between the two points. However, the medial inclination at P3 was significantly different at 16.47° Based on these results, screws should be inserted in a medially inclined rather than vertical direction (Table 8).

Surgical results

Based on this data, upper border fixation was surgically applied to 17 patients (among which 7 had zygomaticomaxillary complex fractures) who presented unstable frac-

Table 4 Distances between G-line and vantage points for rigid fixation with screw insertion.

Variables	P1B($n=25$)	P1A($n=26$)	P2($n=51$)	P3($n=51$)	P4($n=51$)
Mean (mm)	−4.55	1.73	10.43	23.49	37.31
Standard deviation (mm)	3.264	1.420	3.290	2.774	3.110
Standard error (mm)	0.653	0.279	0.461	0.388	0.435
95% CI for the mean (mm)	−(5.89-3.20)	1.15-2.30	9.50-11.35	22.71-24.27	36.43-38.18
Minimal value (mm)	−11.46	0.02	2.99	18.32	26.73
Maximal value (mm)	−0.06	0.02	20.58	33.39	44.08
Significant difference	0.000 (in comparison between any points)				

CI, Confidence intervals; P1B, Point 1 on zygomatic body; P1A, Point 1 on zygomatic arch.

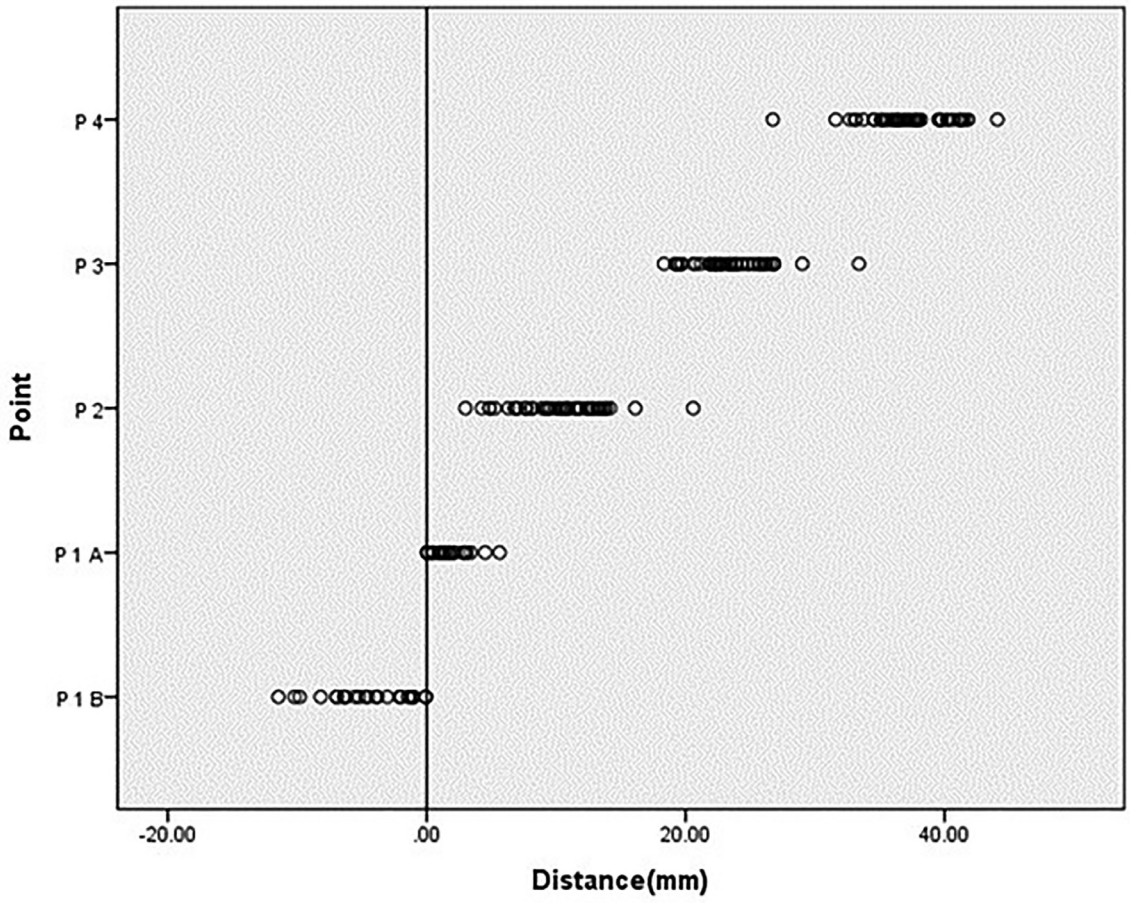

Figure 4 Distances between G-line and vantage points for rigid fixation with screw insertion. The vertical line at 0.0 point represents the G-line. P1B, Point 1 on zygomatic body; P1A, Point 1 on zygomatic arch.

Table 5 Zygomatic arch upper portion thickness.

Variables	P1B($n=25$)	P1A($n=26$)	P2($n=51$)	P3($n=51$)	P4($n=51$)
Mean (mm)	3.03	4.11	1.94	2.40	2.50
Standard deviation (mm)	0.287	0.417	0.118	0.249	0.282
Standard error (mm)	0.057	0.082	0.017	0.035	0.040
95% CI for the mean (mm)	2.92-3.16	3.95-4.28	1.91-1.98	2.33-2.47	2.42-2.58
Minimal value (mm)	2.65	3.06	1.67	1.98	1.72
Maximal value (mm)	3.56	4.86	2.16	2.98	2.89
Significant difference	0.000 (in comparison between any points, except between P3 and P4)				

CI, Confidence intervals; P1B, Point 1 on zygomatic body; P1A, Point 1 on zygomatic arch.

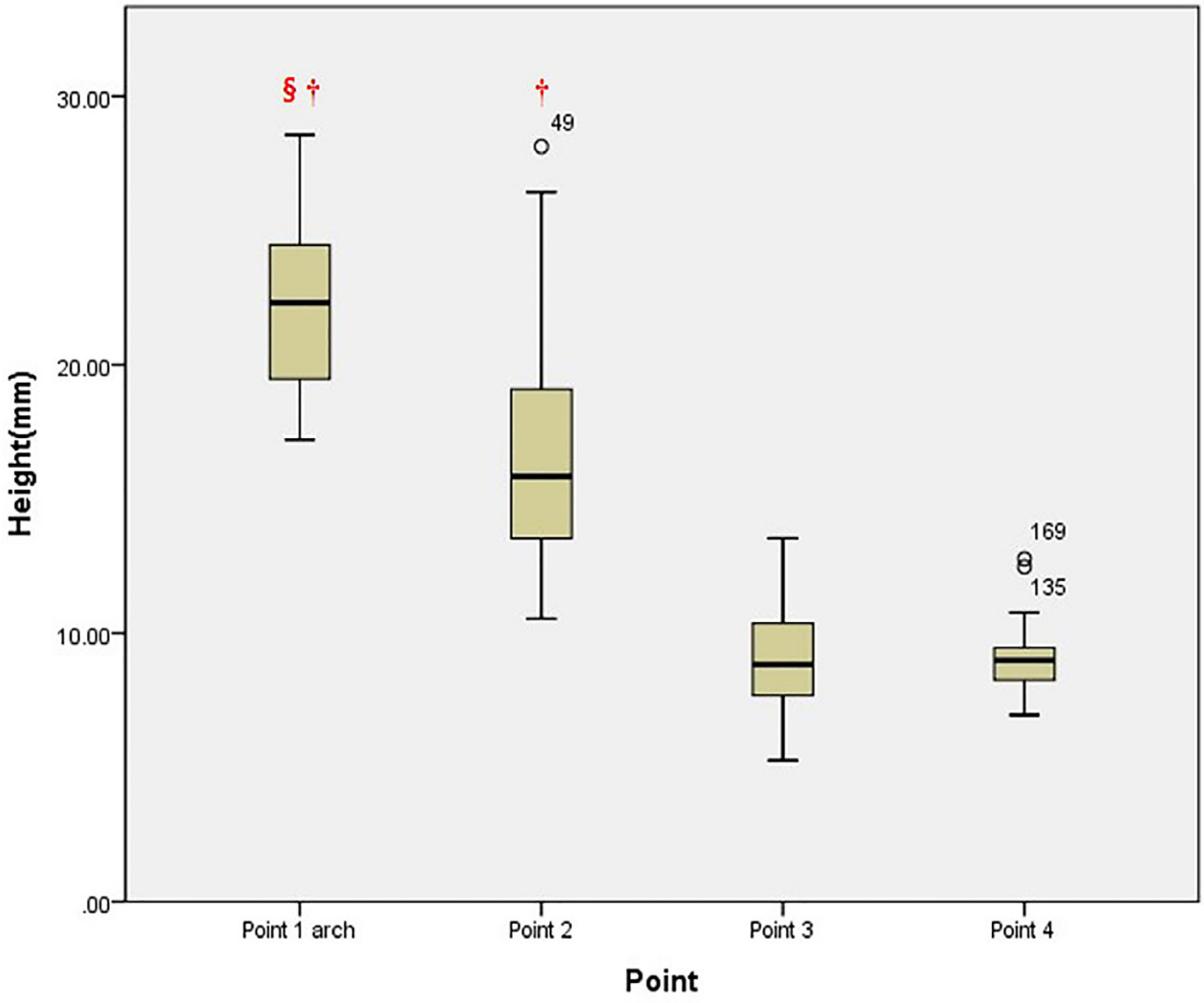

Figure 5 Vertical height of Zygomatic arch at vantage points for rigid fixation. §, significant difference between P2 and P4. †, significant difference between P3 and P4.

Table 6 Zygomatic arch mid-portion thickness.

Variables	P1B($n=25$)	P1A($n=26$)	P2($n=51$)	P3($n=51$)	P4($n=51$)
Mean (mm)	5.50	4.83	3.38	3.96	5.60
Standard deviation (mm)	1.257	0.978	0.520	0.383	0.872
Standard error (mm)	0.251	0.192	0.073	0.054	0.125
95% CI for the mean (mm)	4.99-6.02	4.43-5.22	3.24-3.53	3.85-4.06	5.75-6.25
Minimal value (mm)	3.38	2.98	2.06	3.13	4.00
Maximal value (mm)	7.36	6.48	4.77	4.76	8.30
Significant difference		†	+ §	§	

CI, Confidence intervals; P1B, Point 1 on zygomatic body; P1A, Point 1 on zygomatic arch;
§ Thickness was significantly thinner than in the other three points ($p=0.000$, P1B, P1A, or P4);
† Thickness was significantly thinner than in P4 ($p=0.000$);
+ Thickness was significantly thinner than in P3 ($p=0.000$).

ture reduction including floating segments during conventional procedures from September 2014 to August 2017. Screws of 6 or 8 mm-length were inserted in each fixation point; 6–9 screws were used in comminuted cases (Figure 7), and 5–6 in simple fractures. Operational time averaged 1 h 20 min. A soft diet was recommended for the immediate postoperative period, but regular diets were permitted after one week, and after a 2-week period of limiting mouth opening to a width of 2 finger breadths, free jaw movement was permitted. No significant postoperative

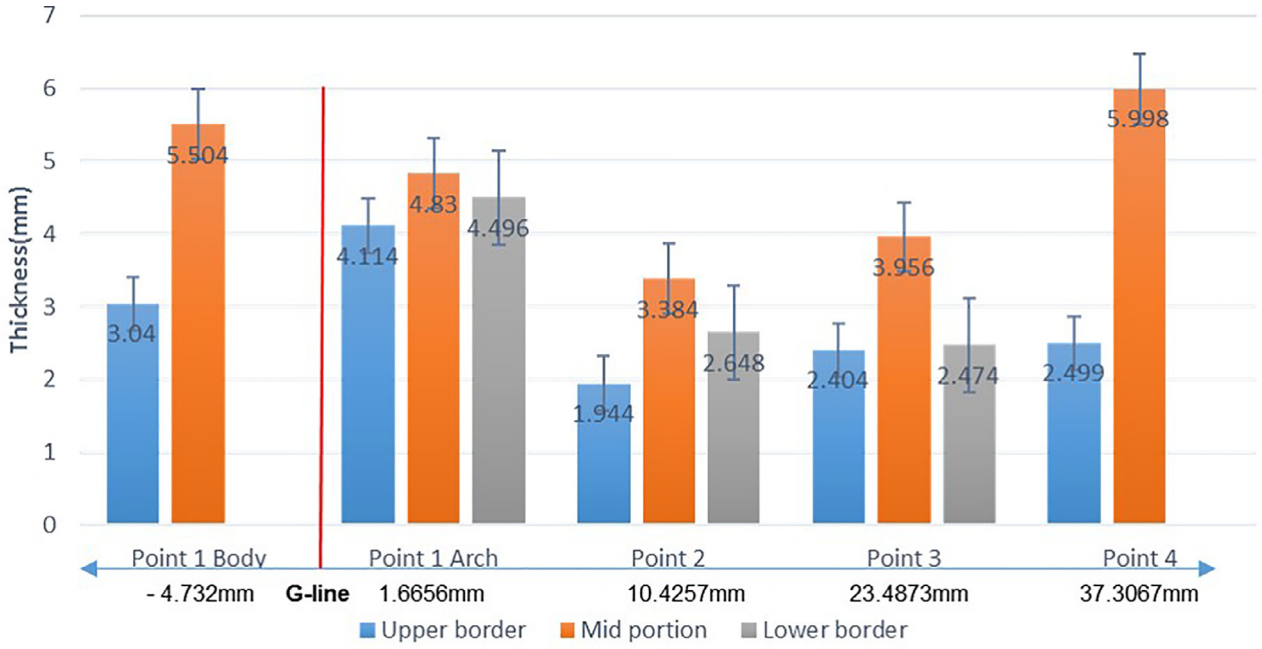

Figure 6 Horizontal thickness of Zygomatic arch at vantage points for rigid fixation. P2 had the least thickness at all vertical levels, with the upper portion being less than 2 mm thick.

Table 7 Zygomatic arch lower portion thickness.

Variables	P1A($n=26$)	P2($n=51$)	P3($n=51$)
Mean (mm)	4.51	2.67	2.47
Standard deviation (mm)	0.325	0.289	0.218
Standard error (mm)	0.064	0.040	0.030
95% CI for the mean (mm)	4.38-4.64	2.57-2.73	2.41-2.54
Minimal value (mm)	4.03	1.93	2.08
Maximal value (mm)	4.95	3.09	2.98
Significant difference		†	§ †

CI, Confidence intervals;
§ Thickness was significantly thinner than in P1A and P2 ($p=0.000$, 0.003);
† Thickness was significantly thinner than in P1A ($p=0.000$).

Table 8 Vertical inclination at vantage points.

Variables	P1A($n=51$)	P2($n=51$)	P3($n=51$)
Mean (°)	6.51	6.61	16.47
Standard deviation (°)	3.64	4.94	6.54
Standard error (°)	0.51	0.69	0.92
95% CI for the mean (°)	5.49-7.53	5.21-7.99	14.63-18.31
Minimal value (°)	1.00	−5.00	3.00
Maximal value (°)	14.00	19.00	32.00
Significant difference			§

CI, Confidence intervals;
§ Vertical inclination was significantly greater than P1A and P2 ($p=0.000$).

complications such as facial nerve injury, trismus, or midface width discrepancies were observed during follow-up periods of at least 6 months. One patient presented hypoesthesia around the incision site for several months, which gradually improved.

Discussion

Fractures of the arch may occur as part of zygomaticomaxillary complex fractures but also as independent injuries resulting from direct impact to the temporolateral facial

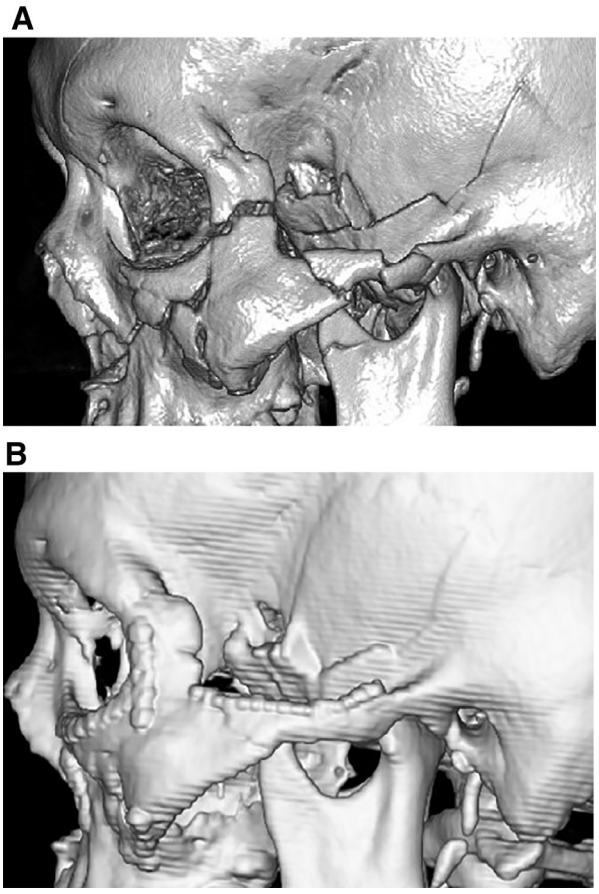

Figure 7 Left Zygomaticomaxillary complex fracture including segmental arch fracture. (A) Comminuted fracture with displaced segment of arch in lateral view of preoperative three-dimensional CT. (B) Open reduction and arch upper border plate fixation in lateral view of three-dimensional CT at postoperative 4 months.

region.[3] Various studies have focused on the morphological findings and management of zygomatic fractures. Although many categorize fracture types based on impact force and direction or displacement patterns,[4,5] some propose a classification system based on the number of fractured segments or whether or not bony contact was maintained between fragments.[2,6,7] Differences in classification philosophies notwithstanding, the classic Gillies or Keen methods are used for most arch fractures, providing stable reduction in cases with a small number of fracture segments and intact surrounding tissue.[8]

However, studies on frequently fractured locations and their correlation with morphometry dimensions are hard to find. Likewise, classical methods are unsatisfactory for unstable floating segments or laterally displaced fractures. The coronal approach has its own drawbacks, while less invasive methods using K-wires or lag screws do not always provide a direct view of the fracture, leading to uncertain results.[9,10]

The surgical method introduced in this study applies osteosynthetic material to the upper arch surface in order to overcome these problems. The morphometry analysis provides the basis for this method, especially concerning frequent fracture locations, application of hardware, and surgical approach.

The first significance of this study is that morphometric analysis was performed to verify the locations of frequently fractured sites and the practicality of rigid fixation through tangential hardware application. Although the fact that only typical M-shaped fractures with two segments were included is a limitation, the results state that the arch is most frequently fractured 4.40, 10.95 and 24.3 mm posterior to its virtual origin. The arch had the least vertical height 27.09 mm behind its origin, which was not correlated to any of the frequent fracture sites. Song et al have reported that the horizontal thickness of the arch was fairly consistent along its length at about 3.5 mm, and that the most laterally prominent region had the least thickness.[11] The results of this study concur that the central portion of the arch is generally thinner, with the thinnest point 12.23 mm posterior to the G-line. The vertical midportion is also thicker than the upper border portion along the whole arch length; screws applied correctly to the upper surface would be safely embedded in bone without protrusion.

The second significant point of this study is that hardware is tangentially applied to the upper border of the arch. Regardless of the approach, conventional methods for unstable arch fracture management involved applying osteosynthetic material to the outer cortex.[12-14] While the coronal approach would allow upper surface tangential fixation, to the best of the authors' knowledge, this method has not been reported before. Plates applied to the lateral cortex can be palpated through the skin, and thick plates can also increase facial width. Tangential upper surface fixation can avoid these complications. Periosteal dissection is also limited to a small area of the upper border, which may help enhance bone healing. Biomechanically speaking, upper border fixation may be less stable than fixation to the outer cortex considering muscle movement; however, only a limited portion of the masseter muscle affects the arch, and additional screws can adequately resist this force.

The third significance of this study is that a temporal hairline incision was used. This provides a direct view of the fracture for precise anatomical reduction and fixation. The range of dissection is much smaller than with the coronal approach. The short incision placed inside the hair-bearing scalp leaves an inconspicuous scar. Other less-invasive approaches such as preauricular or intraoral incisions can also be used for fixation, but the view provided by these incisions is frequently insufficient for fixation, therefore requiring the assistance of additional equipment; even so, hardware can only be applied to the outer cortex.

Some precautions are necessary when using this method. Cicatrical alopecia or dysaesthesia can occur around the incision, and temporal hollowing also is a potential complication. A beveled incision parallel to the temporal hair follicles and limited use of electrocautery hemostasis can minimize follicular damage and subsequent alopecia. The skin around the incision site is innervated by the zygomaticotemporal nerve, which emerges through the superficial layer of the deep temporal fascia 15 mm posterior to the frontozygomatic suture and 20 mm superior to the upper margin of

the arch, with a horizontal branch extending laterally to connect with branches of the auriculotemporal nerve.[15-17] The anterior portion of the incision should be placed slightly superior-posterior to this area. The frontotemporal branch of the facial nerve should be preserved in the same method as in a coronal approach, taking care to avoid excessive traction. Temporal hollowing can be prevented by securely restoring integrity of each fascial layer,[18] which is also important for postoperative fracture segment stability and bony union.

According to the morphometric study, the thinnest portion of the arch is 12.23 mm behind its origin, which should be kept in mind. Screws 6 or 8 mm long would be appropriate to ensure an insertion length reaching at least half of the arch height. The authors' recommended fixation sequence begins with selecting a plate of appropriate length and molding its contour to the non-injured contralateral arch. The anterior and posterior non-fractured portions are fixated first, after which the central fractured segments are fixated.

There were some limitations to this study. Force of impact was not evaluated when investigating frequent fracture points, as the study subjects were actual patients. Potential discrepancies between CT image evaluation and actual bone measurements was also an issue. However, recent multi-slice CT with multiple detector arrays (64 rows) provide reduced artifacts and sub-millimeter resolution up to 0.4 mm isotropic voxel, resulting in an accuracy over 90% in displaying linear fractures, and this was deemed sufficient for this study.[19,20]

Conclusions

The authors' novel method can provide immediate anatomical reduction and rigid fixation in arch fractures where closed reduction methods would likely produce poor results. Internal fixation can reduce the period of diet and jaw opening limitation, and morbidity is less compared to the coronal approach. In this sense, this study introduces a new method of open reduction and internal fixation for zygomatic arch fractures, validated by morphometric analysis of the arch for tangential plate application. A prospective study series including objective cadaver evaluation methods should be performed in the future for stronger evidence.

Funding

None.

Conflicts of interest statement

None to declare.

Ethical approval

Research protocol was approved by the local Ethical Committee (Korea University institutional review board, K2017-3229).

Video 1. Surgical Procedure of Open Reduction with Upper Border Plate Fixation.

Supplementary materials

Supplementary material associated with this article can be found, in the online version, at doi:10.1016/j.bjps.2018.11.014.

References

1. Ogden GR. The Gillies method for fractured zygomas: An analysis of 105 cases. *J Oral Maxillofac Surg* 1991;**49**(1):23-5.
2. Ozyazgan I, Gunay GK, Eskitascioglu T, et al. A new proposal of classification of zygomatic arch fractures. *J Oral Maxillofac Surg* 2007;**65**(3):462-9.
3. Czerwinski M, Ma S, Williams HB. Zygomatic arch deformation: An anatomic and clinical study. *J Oral Maxillofac Surg* 2008;**66**(11):2322-9.
4. Knight JS, North JF. The classification of malar fractures: an analysis of displacement as a guide to treatment. *Br J Plast Surg* 1961;**13**:325-39.
5. Czerwinski M, Lee C. Traumatic arch injury: indications and an endoscopic method of repair. *Facial Plast Surg* 2004;**20**(3):231-8.
6. Yamamoto K, Murakami K, Sugiura T, et al. Clinical analysis of isolated zygomatic arch fractures. *J Oral Maxillofac Surg* 2007;**65**(3):457-61.
7. Kim J, Kim S, Chung S, et al. Zygomatic arch fracture: A new classification and treatment algorithm with epidemiologic analysis. *J Craniofac Surg* 2014;**25**(4):1389-92.
8. Hindin DI, Muetterties CE, Mehta C, et al. Treatment of Isolated Zygomatic Arch Fracture: Improved Outcomes with External Splinting. *Plast Reconstr Surg* 2017;**139**(5):1162e-1171e.
9. Camilleri AC, Gilhooly M, Cooke ME. Stabilisation of the unstable fractured zygomatic arch with a Kirschner wire. *Br J Oral Maxillofac Surg* 2005;**43**(2):183-4.
10. de Santana Santos T, da Rocha Neto AM, Medeiros R Jr, et al. Treatment of zygomatic arch fracture with lag screws. *J Craniofac Surg* 2011;**22**(4):1468-70.
11. Song WC, Choi HG, Kim SH, et al. Topographic anatomy of the zygomatic arch and temporal fossa: a cadaveric study. *J Plast Reconstr Aesthet Surg* 2009;**62**(11):1375-8.
12. Krimmel M, Cornelius CP, Reinert S. Endoscopically assisted zygomatic fracture reduction and osteosynthesis revisited. *Int J Oral Maxillofac Surg* 2002;**31**(5):485-8.
13. Xie L, Shao Y, Hu Y, et al. Modification of surgical technique in isolated zygomatic arch fracture repair: Seven case studies. *Int J Oral Maxillofac Surg* 2009;**38**(10):1096-100.
14. Swanson E, Vercler C, Yaremchuk MJ, et al. Modified Gillies approach for zygomatic arch fracture reduction in the setting of bicoronal exposure. *J Craniofac Surg* 2012;**23**(3):859-62.
15. Hwang K, Suh MS, Lee SI, et al. Zygomaticotemporal nerve passage in the orbit and temporal area. *J Craniofac Surg* 2004;**15**(2):209-14.
16. Totonchi A, Pashmini N, Guyuron B. The zygomaticotemporal branch of the trigeminal nerve: an anatomical study. *Plast Reconstr Surg* 2005;**115**(1):273-7.
17. Lei T, Gao JH, Xu DC, et al. The frontal-temporal nerve triangle: A new concept of locating the motor and sensory nerves in upper third of the face rhytidectomy. *Plast Reconstr Surg* 2006;**117**(2):385-94.
18. Matic DB, Kim S. Temporal hollowing following coronal incision: a prospective, randomized, controlled trial. *Plast Reconstr Surg* 2008;**121**(6):379e-385e.

19. William CS. Imaging of maxillofacial trauma: Evolutions and emerging revolutions. *Oral Surg Oral Med Oral Pathol Oral Radiol Endod* 2005;**100**(2):S75–96.

20. Eskandarlau A, Poorolajal J, Talaeipour AR, et al. Comparison between cone beam computed tomography and multislice computed tomography in diagnostic accuracy of maxillofacial fractures in dried human skull: an in vitro study. *Dent Traumatol* 2014;**30**(2):162–8.